J. Phys. Chem. A **2005,** *109,* 4881−4890

Photoinduced Electron Transfer in Double-Bridged Porphyrin−Fullerene Triads

Marja Isosomppi,* Nikolai V. Tkachenko, Alexander Efimov, and Helge Lemmetyinen

Institute of Materials Chemistry, Tampere University of Technology, P.O. Box 541, 33101 Tampere, Finland

Received: February 28, 2005; In Final Form: April 19, 2005

Electron and energy transfer reactions of porphyrin−porphyrin−fullerene triads (P_2P_1C) with controllable sandwich-like structures have been studied using spectroscopic and electrochemical methods. The stabile, stacked structure of the molecules was achieved applying a two-linker strategy developed previously for porphyrin−fullerene dyads. Different triad structures with altered linker positions, linker lengths, and center atoms of the porphyrin rings were studied. The final charge-separated (CS) state and the different transient states of the reactions have been identified and energies of the states estimated based on the experimental results. In particular, a complete CS state $P_2^+P_1C^-$ was achieved in a zinc porphyrin−free-base porphyrin−fullerene triad (**ZnP$_2$t9P$_1$C**) in both polar (benzonitrile) and nonpolar (toluene) solvents. The lifetime of this state was longer living in the nonpolar solvent. An outstanding feature of the **ZnP$_2$t9P$_1$C** triad is the extremely fast formation of the final CS state, $P_2^+P_1C^-$. This state is formed after primary excitation of either zinc porphyrin or free-base porphyrin chromophores in less than 200 fs. Although the intermediate steps between the locally excited states and the final CS state were not time-resolved for this compound, the process is clearly multistep and the fastest ever observed for porphyrin-based compounds.

1. Introduction

There are two somewhat contradictory aims in designing molecules capable of solar energy conversion. First, the charge separation reaction should occur efficiently and controllably, and second, the CS state should have a long-enough lifetime to be utilized in solar cells or the like. Essential for the fast and efficient electron transfer (ET) is the small reorganization energy of the reaction, and the Marcus theory predicts that the reorganization energy becomes smaller as the distance between the electron donor and acceptor decreases.[1] In fact, it has been experimentally proven that efficient charge separation is achieved in molecules where the electron donor and acceptor moieties are in close, face-to-face contact.[2,3] However, also the back-electron transfer is fast for these compounds, resulting in a too short period of time to utilize the potential of the CS state. This problem could be solved by designing molecules in which the charge separation proceeds in several short distance steps. This way there is a long distance between the charges in the final CS state retarding the back-electron transfer and still the reaction takes place efficiently.

Different systems consisting of porphyrins as electron donors and fullerenes as acceptors have been the targets of interest for many research groups focusing on photoinduced ET during the past decade. Especially, porphyrin−fullerene dyads, in which the two chromophores are linked covalently together, have been studied extensively.[2c,4] Also more complex structures, combining several porphyrin moieties or other secondary electron donors to the porphyrin−fullerene dyad, and their stepwise charge separation reactions have been reported.[4i−k,5] In these compounds, the different moieties are fixed together with a single linker, and the advantageous face-to-face contact of the electron donors and acceptors is necessarily not obtained. To achieve a more stable structure, in which charge separation occurs to a desired direction in controlled time, two-linker strategies have been developed for porphyrin-fullerene dyads.[3,6,7] In these systems, porphyrin is attached to fullerene with two linkers keeping the structure stable and organized. This is of special interest when the compounds are applied in solid-state devices, where the molecules can be organized to attain electric current in a specified direction.

The strategy of the present study was to combine the advantages of the long distance of the CS state and the organized sandwich-like structure by attaching a second porphyrin to the double-bridged porphyrin−fullerene dyad[7] to act as a secondary electron donor. The target of this approach was to prolong the CS state achieved earlier with the dyads.[3] Also the second porphyrin was attached with two linkers to form a stacked triad structure. Different triad structures with altered linker positions, linker lengths, and center atoms of the porphyrin rings were studied. We report here on the study of the photodynamics of these new triads in polar (benzonitrile) and nonpolar (toluene) solvents. The different transient states of the photoinduced ET reaction were identified and their lifetimes determined using both the steady-state and time-resolved spectroscopic methods. The energy levels of the observed CS states were estimated from differential pulse voltametric (DPV) measurements.

We found that substituting a Zn-ion as the center atom of the side porphyrin P_2 of the triad (**ZnP$_2$t9P$_1$C**) provides a potential energy gradient for ET from Zn porphyrin to the adjacent free-base porphyrin−fullerene moiety. The formation of the complete CS state of this triad was so fast that the possible intermediates could not be resolved. Furthermore, it seems that the complete CS state can be achieved even in a nonpolar solvent such as toluene. Instead, the otherwise similar triad having free-base porphyrin as the secondary electron donor behaves very similarly as the corresponding dyad studied earlier.[3]

---

* To whom correspondence should be addressed. E-mail: marja.isosomppi@tut.fi.

10.1021/jp051011n CCC: $30.25

SCHEME 1: Synthesis of the Compounds[a]

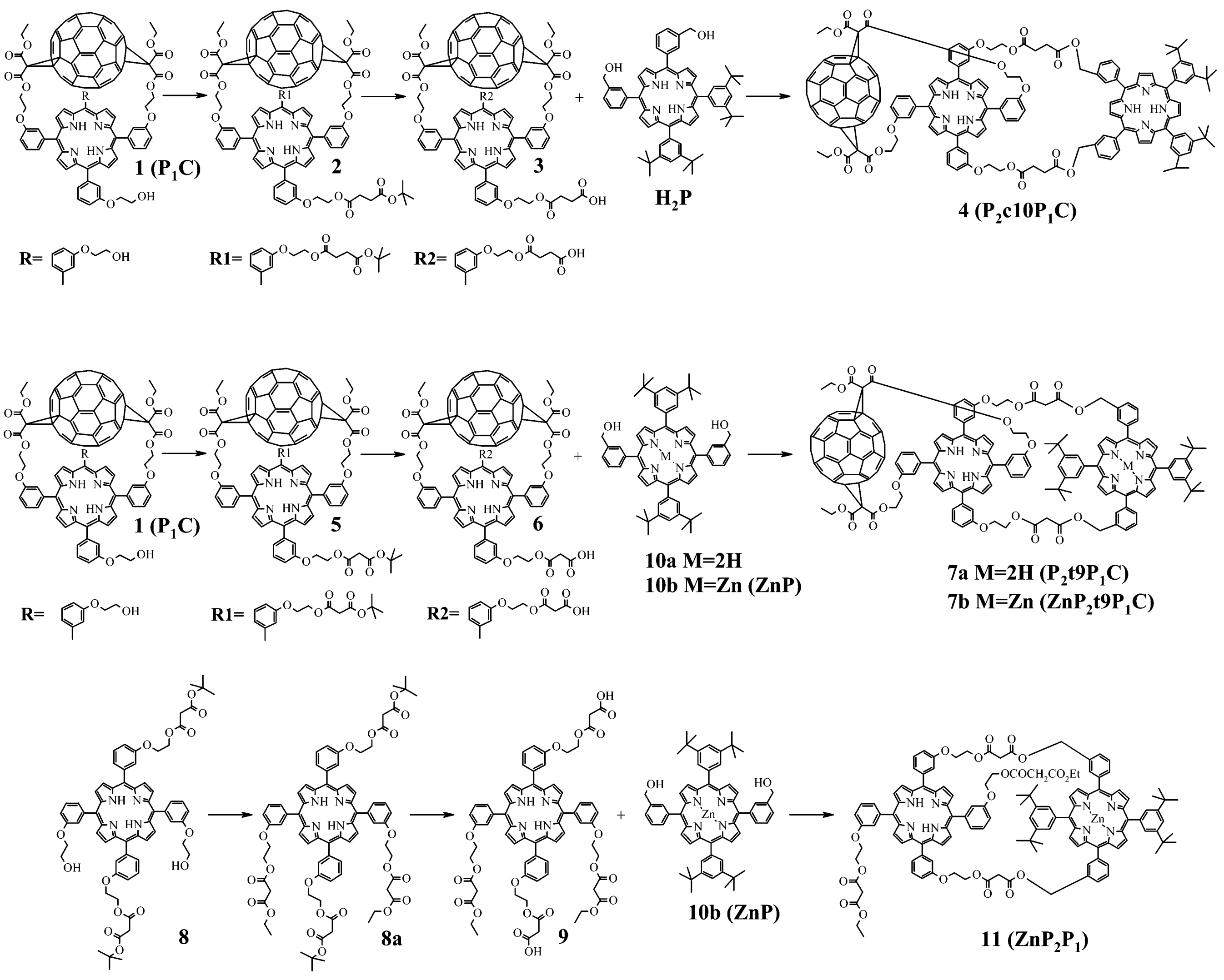

[a] The abbreviations: P_1 = first porphyrin, the one closest to fullerene; P_2 = second porphyrin of the molecule; C = C_{60}-fullerene; c, t = cis (5, 10) or trans (5, 15) position of the linkers in P_2, respectively; 9, 10 = number of atoms in the linkers between P_1 and P_2.

2. Materials and Methods

2.1. Studied Compounds. The structures of the studied compounds and the synthetic routes are presented in Scheme 1.

The compounds **1** (**P_1C**), **8**, **10a**, **10b** (**ZnP**), and **H_2P** were prepared as described earlier.[3,7] The solvents used in the synthesis and separations were distilled prior to use. Buckminsterfullerene C_{60} (>98%) was purchased from Fluka (Buchs, Switzerland).

The ^1H NMR spectra were run on a 300 MHz Varian Mercury spectrometer. Mass spectra were measured using a Fourier transform ion cyclotron resonance mass spectrometer, Bruker BioApex47e.

2.1.1. Synthesis of ***P_2c10P_1C***. A total of 10 mg (0.0056 mmol) of dyad **1** (**P_1C**), 4.2 mg (0.024 mmol) of mono-*tert*-butyl succinate, 5 mg (0.024 mmol) of dicyclohexylcarbodiimide, and 0.5 mg of *N*,*N*-dimethylaminopyridine were stirred in 30 mL of dichloromethane at r.t. for 48 h. The precipitate of cyclohexylurea was filtered off, and the product was purified on Silica 60 column (eluted with chloroform) to yield 10 mg (84%) of compound **2**. ^1H NMR (300 MHz, $CDCl_3$) δ_H: 8.83−8.60 (m, 8H, β-*H*), 8.30−8.23 (m, 2H, phenyl-*H*), 7.87−7.17 (m, 14H, phenyl-*H*), 5.23−5.09 (m, 2H, OCH_2CH_2O), 4.84−4.71 (m, 2H, OCH_2CH_2O), 4.62−3.78 (m, 16H, OCH_2CH_2O, OCH_2CH_3), 2.75−2.48 (m, 8H, $O_2CCH_2CH_2CO_2$), 1.45−1.38 (m, 24H, OCH_2CH_3, *tert*-butyl-*H*), −3.03 (s, 2H, N*H*).

Compound **2** was dissolved in 5 mL of trifluoroacetic acid and stirred at r.t. for 12 h. The reaction mixture was diluted with 2 mL of toluene and evaporated under reduced pressure at 30 °C. The green dry residue was dissolved in 20 mL of dichloromethane, washed with 100 mL of water (3 times), dried over anhydrous sodium sulfate, and evaporated to yield quantitatively compound **3**.

A total of 5.8 mg (0.0029 mmol) of dyad **3**, 3 mg (0.0033 mmol) of porphyrin **H_2P**, 2 mg (0.0097 mmol) of dicyclohexylcarbodiimide, and 1.5 mg of *N*,*N*-dimethylaminopyridine were dissolved in 6 mL of dichloromethane, stirred at 0 °C for 30 min, and then stirred at r.t. for 24 h. The separation of the reaction products was done by column chromatography on Silica 60 (eluted with dichloromethane). The first red-brown band was collected to yield 2.8 mg (34%) of the target triad **4** (**P_2c10P_1C**). ^1H NMR (300 MHz, $CDCl_3$) δ_H: 8.97−8.42 (m, 16H, β-*H*), 8.23−6.64 (m, 30H, phenyl-*H*), 5.53−4.81 (m, 8H, OCH_2CH_2O, $Ar-CH_2$), 4.63−3.57 (m, 16H, OCH_2CH_2O, OCH_2CH_3), 2.89−2.27 (m, 8H, $O_2CCH_2CH_2CO_2$), 1.66−1.41 (m, 42H, *tert*-butyl-*H*, OCH_2CH_3), −2.69 to −3.35 (m, 4H, N*H*). UV−Vis (toluene), λ_{max} (ϵ): 425 (330000), 518 (19100), 552 (9200), 596

(5600), 650 (4000). MS (MALDI-DHB): 2863.91 $[M+H]^+$; calcd for $C_{192}H_{124}N_8O_{20}$: 2863.17.

2.1.2. Synthesis of ***P_2t9P_1C*** *and* ***ZnP_2t9P_1C***. A total of 11 mg (0.006 mmol) of dyad **P_1C**, 10 mg (0.04 mmol) of 2-chloro-*N*-methyl-pyridinium iodide, 6.1 μL (6.4 mg, 0.04 mmol) of mono-*tert*-butyl malonate, and 11.2 μL (8.1 mg, 0.08 mmol) of triethylamine were stirred in 10 mL of dichloromethane at r.t. for 12 h. Another 5 mg of 2-chloro-*N*-methyl-pyridinium iodide, 3 μL of mono-*tert*-butyl malonate, and 5 μL of triethylamine were added, and the reaction mixture was stirred for an additional 12 h. The red solution was poured into 30 mL of water, the organic layer was separated, washed with water (3 × 50 mL), dried over anhydrous sodium sulfate, and evaporated to yield 11.6 mg (88%) of the dyad **5**. The product was used in the next step without further purification. ^{1}H NMR (300 MHz, $CDCl_3$) δ_H: 8.83−8.62 (m, 8H, β-*H*), 8.36−8.17 (m, 2H, phenyl-*H*), 7.88−7.17 (m, 14H, phenyl-*H*), 5.23−5.09 (m, 2H, OCH_2CH_2O), 4.84−4.71 (m, 2H, OCH_2CH_2O), 4.65−4.07 (m, 16H, OCH_2CH_2O, OCH_2CH_3), 3.33 (s, 4H, O_2CCH_2-CO_2), 1.49−1.44 (m, 24H, *tert*-butyl-*H*, OCH_2CH_3), −3.02 (s, 2H, N*H*).

Compound **5** was dissolved in 2 mL of trifluoroacetic acid and stirred at r.t. for 12 h. The reaction mixture was diluted with 30 mL of chloroform, washed with water (5 × 100 mL), dried over anhydrous sodium sulfate, and evaporated to yield quantitatively compound **6**.

The dyad **6** (approximately 0.006 mmol) was dissolved in 15 mL of dichloromethane, then 7.7 mg (0.03 mmol) of 2-chloro-*N*-methyl-pyridinium iodide, 6.1 μL (6.4 mg, 0.04 mmol) of mono-*tert*-butyl malonate, 8.4 μL (6 mg, 0.06 mmol) of triethylamine, and 9 mg (0.01) of porphyrin **10a** were added, and the reaction mixture was stirred for 16 h. The solution was diluted with 30 mL of dichloromethane and washed with 100 mL of water, and the organic layer was separated, dried over anhydrous sodium sulfate, and evaporated to dryness. The triad was separated first on Silica 60 column (gradient elution toluene/ethyl acetate 50/1−25/1) by collecting second brown-red zone. Further purification was performed on Merck Silica gel 60 HPTLC plates in chloroform to yield 4.1 mg (29%) of the triad **7a** (**P_2t9P_1C**). ^{1}H NMR (300 MHz, $CDCl_3$) δ_H: 8.67−8.45 (m, 16H, β-*H*), 8.14−8.01 (m, 4H, phenyl-*H*), 7.99−7.75 (m, 6H, phenyl-*H*), 7.73−7.52 (m, 6H, phenyl-*H*), 7.32−7.27 (m, 2H, phenyl-*H*), 7.23−7.12 (m, 6H, phenyl-*H*), 5.40 (s, 4H, Ar−CH_2), 4.93−4.68 (m, 2H, OCH_2CH_2O), 4.57−3.80 (m, 18H, OCH_2CH_2O, OCH_2CH_3), 3.14 (s, 4H, $O_2CCH_2CO_2$), 1.46 (s, 18H, *tert*-butyl-*H*), 1.45 (s, 18H, *tert*-butyl-*H*), 1.33−1.27 (m, 6H, OCH_2CH_3), −3.22 to −3.48 (m, 4H, N*H*). UV−Vis (toluene), λ_{max} (ϵ): 427 (399000), 519 (28400), 553 (16700), 595 (10500), 651 (7000). MS (MALDI-DHB): 2835.87 $[M+H]^+$; calcd for $C_{190}H_{120}N_8O_{20}$: 2835.12.

The triad **7b** (**ZnP_2t9P_1C**) was prepared the same way as compound **7a** by reaction of the dyad **6** and metal complex **10b** (**ZnP**) with 14% yield. ^{1}H NMR (300 MHz, $CDCl_3$) δ_H: 8.82−8.40 (m, 16H, β-*H*), 8.15−8.02 (m, 4H, phenyl-*H*), 7.99−7.75 (m, 6H, phenyl-*H*), 7.73−7.52 (m, 6H, phenyl-*H*), 7.41−7.29 (m, 2H, phenyl-*H*), 7.24−7.10 (m, 6H, phenyl-*H*), 5.40 (s, 4H, Ar−CH_2), 4.96−4.82 (m, 2H, OCH_2CH_2O), 4.61−3.84 (m, 18H, OCH_2CH_2O, OCH_2CH_3), 3.13 (s, 4H, $O_2CCH_2CO_2$), 1.46 (s, 36H, *tert*-butyl-*H*), 1.32−1.28 (m, 6H, OCH_2CH_3), −3.45 (s, 2H, N*H*). UV−Vis (toluene), λ_{max} (ϵ): 429 (444000), 518 (16200), 552 (23300), 593 (8800), 651 (3700). MS (MALDI-DHB): 2899.78 $[M+H]^+$; calcd for $C_{190}H_{118}N_8O_{20}Zn$: 2898.47.

2.1.3. Synthesis of ***Zn$P_2$$P_1$***. 23 mg (0.02 mmol) of porphyrin **8** and 5.9 μL (4.2 mg, 0.042 mmol) of triethylamine were dissolved in 7 mL of dichloromethane, then 5.4 μL (6.3 mg, 0.042 mmol) of ethyl malonyl chloride were added, and the reaction mixture was stirred for 12 h. The solvent was evaporated, and the dry residue of porphyrin **8a** was dissolved in 3 mL of trifluoroacetic acid. The green solution was stirred at r.t. for 10 h, diluted with 20 mL of chloroform, and washed with water (3 × 100 mL). The red organic solution was evaporated, and the residue was dried in vacuo to yield 20 mg (79%) of porphyrin **9**.

A total of 20 mg (0.0159 mmol) of porphyrin **9**, 15.4 mg (0.0159 mmol) of metal complex **10b** (**ZnP**), and 13.3 mg (0.051 mmol) of 2-chloro-*N*-methylpyridinium iodide were dissolved in 20 mL of dichloromethane. A total of 13.3 μL (6 mg, 0.06 mmol) of triethylamine were added, and the solution was stirred at r.t. for 18 h. The solution was diluted with 30 mL of dichloromethane and washed with 100 mL of water, and the organic layer was separated, dried over anhydrous sodium sulfate, and evaporated to dryness. The dyad was separated on Silica 60 column (gradient elution chloroform − chlorofom/dichloromethane 1/1) by collecting first brown-red zone. Further purification was performed on Merck Silica gel 60 HPTLC plates in chloroform to yield 7.2 mg (21%) of the dyad **11** (**Zn$P_2$$P_1$**). ^{1}H NMR (300 MHz, $CDCl_3$) δ_H: 9.02−8.59 (m, 16H, β-*H*), 8.56−7.51 (m, 24H, phenyl-*H*), 7.47−6.62 (m, 6H, phenyl-*H*), 5.49−5.06 (m, 4H, Ar−CH_2), 4.63−3.77 (m, 20H, OCH_2CH_2O, OCH_2CH_3), 3.49−3.24 (m, 8H, $O_2CCH_2CO_2$), 1.47−1.23 (m, 42H, *tert*-butyl-*H*, OCH_2CH_3), −2.59 to −3.32 (br, 2H, N*H*). UV−Vis (toluene), λ_{max} (ϵ): 420 (535000), 515 (14700), 551 (21100), 591 (6800), 647 (1800). MS (MALDI-DHB): 2181.74 $[M]^+$; calcd for $C_{130}H_{122}N_8O_{20}Zn$: 2181.83.

2.2. Spectroscopic Methods. All of the spectroscopic measurements were carried out both in benzonitrile (PhCN) and in toluene representing polar and nonpolar environments, respectively.

The steady-state absorption spectra of the compounds were measured with a Shimadzu UV-2501PC spectrophotometer. Steady-state fluorescence spectra were recorded using a Fluorolog 3 (SPEX Inc.) fluorimeter with a cooled infrared sensitive photomultiplier (Hamamatsu R2658). The emission spectra were corrected using a correction spectrum supplied by the manufacturer.

A time-correlated single photon counting (TCSPC) method was used for the time-resolved fluorescence measurements in the nanosecond and subnanosecond time-scales as described elsewhere.[8] The excitation wavelength was 590 nm and the time resolution about 100 ps (fwhm). Up-conversion and pump−probe techniques for fluorescence and absorption, respectively, were used to detect the fast processes with a time resolution shorter than 0.2 ps. The excitation wavelength was 420 nm for both of these measurements. The instruments and the used data analysis procedure have been described earlier.[8b,9] In addition, the transient absorption measurements with the pump−probe method were done using excitation wavelengths 515 and 555 nm. The different wavelengths were achieved by using an optical parametric amplifier (CDP 2017, CDP Inc., Russia) after multipass femtosecond amplifier and mixing base harmonic with signal or idle beams of the parametric amplifier.

2.3. Differential Pulse Voltammetry. A differential pulse voltammetry was used to estimate the energies of the CS states of the triads. The oxidation potentials of donor porphyrins and the reduction potential of acceptor fullerene were measured with DPV using Ag/AgCl as a pseudo-reference electrode and the energies of the CS states were calculated from the differences between them. 200 μL of 0.1 M tetra-*n*-butylammonium

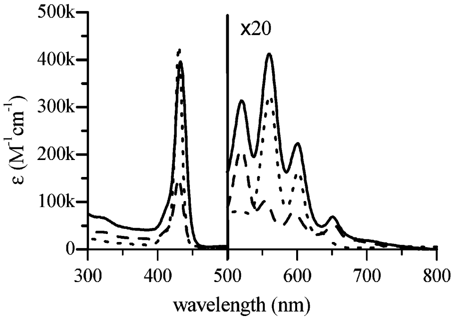

Figure 1. Absorption spectrum of **ZnP_2t9P_1C** in PhCN (solid line). The spectra of the reference dyad **P_1C** (dashed line) and porphyrin **ZnP** (dotted line) are also given for comparison.

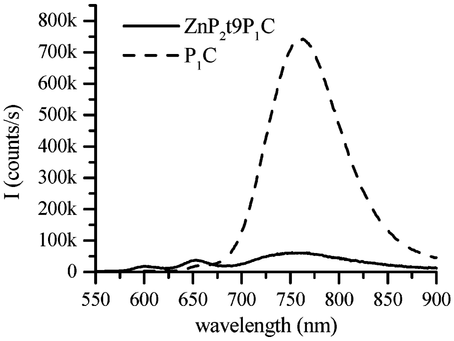

Figure 2. Comparison of the emission spectra of **ZnP_2t9P_1C** and **P_1C** in toluene with excitation wavelength 428 nm.

tetrafluoroborate ($TBABF_4$) in PhCN was used as the supporting electrolyte and the background was measured in a nitrogen flow. After measuring the background, a PhCN solution of the sample was added to the electrochemical cell. The concentrations of the samples in the cell were 0.33−0.34 mM. Finally, the measurements were repeated after adding 20 μL of 2.69 mM ferrocene/PhCN. The measurements were carried out in both directions: toward the positive and negative potential. The reduction and oxidation potentials were calculated as an average of the two scans.

3. Results and Discussion

3.1. Steady-State Measurements. The steady-state absorption spectra of all of the triads indicated some interactions between the porphyrin−fullerene dyad P_1C and side porphyrin P_2. The spectra of the triads were approximately superpositions of the spectra of the dyad and the porphyrin references, but for example, the Soret band was weaker and slightly shifted to the red (**ZnP_2t9P_1C** in PhCN as an example in Figure 1).

The emission spectra of the triads showed that the porphyrin−fullerene moiety P_1C preserves its exciplex nature as it was observed for the corresponding dyad compounds[3]. Emission of the exciplex $(P_1C)^*$ in the region 700−950 nm was observed for all of the triads in nonpolar solvents. However, the exciplex was weaker in the triads compared to the dyad **P_1C**.

Figure 2 clearly demonstrates the quenching of the exciplex in the triad **ZnP_2t9P_1C** compared to the dyad **P_1C**. The intensity of the exciplex emission band at 760 nm is roughly 12 times weaker in the triad. This indicates that the exciplex transforms into another transient, presumably to a CS state, more efficiently in the triad. The quenching of the exciplex was not as significant in the free-base triads **P_2t9P_1C** and **P_2c10P_1C**, where the emissions were only about 1.5 times weaker compared to the dyad, being somewhat more efficient for **P_2t9P_1C** than for **P_2c10P_1C** (Figure S1 of the Supporting Information). This suggests that the exciplex interacts more willingly with the P_2 unit in **P_2t9P_1C** than with P_2 in **P_2c10P_1C**. Moreover, the linker positions in P_2 play an important role also in the energy transfer between the porphyrins of the triad: a considerable difference in the porphyrin monomer emission can be seen between **P_2c10P_1C** and **P_2t9P_1C**. Somewhat shorter linker lengths and especially the more compact sandwich-like structure, achieved with the trans positions of the linkers in **P_2t9P_1C**, result in a more efficient energy transfer from P_2 to P_1 indicated by roughly 2.5 times stronger quenching of the porphyrin monomer emission around 650 and 720 nm.

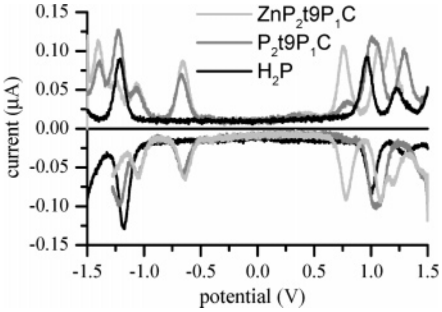

Figure 3. Differential pulse voltammograms of **ZnP_2t9P_1C**, **P_2t9P_1C** and **H_2P** in PhCN, vs pseudo-reference electrode Ag/AgCl. (In measurements with ferrocene in the solution the oxidation peak of ferrocene was observed at 0.45 V.)

TABLE 1: Energies (eV) of the Excited States Obtained from the Emission Spectra in Toluene

	P_2^*	P_1^*	$(P_1C)^*$
P_2c10P_1C	1.90	1.90	1.73
P_2t9P_1C	1.90	1.90	1.70
ZnP_2t9P_1C	2.05	1.90	1.79

TABLE 2: Energies (eV) of the CS States for the Triads Calculated from the DPV Measurements in PhCN

	$P_2^+P_1^-C$	$P_2P_1^+C^-$	$P_2^+P_1C^-$
P_2c10P_1C		1.63	1.67
P_2t9P_1C		1.68	1.73
ZnP_2t9P_1C	2.01	1.72	1.42

The energy levels of the singlet excited states of porphyrins and the exciplexes were obtained from the steady-state emission spectra of the triads (Table 1).

3.2. Voltametric Studies. Figure 3 presents the differential pulse voltammograms for **ZnP_2t9P_1C**, **P_2t9P_1C**, and **H_2P**. The energies of the CS states calculated from the peak positions are presented in Table 2 for the three triads studied.

Comparing the calculated values of $P_2P_1^+C^-$ and $P_2^+P_1C^-$ for the different triads, we can see that for the free-base triads **P_2c10P_1C** and **P_2t9P_1C** transition $P_2P_1^+C^- \rightarrow P_2^+P_1C^-$ is endergonic and therefore the relaxation to the ground state rather occurs directly from $P_2P_1^+C^-$ without going through $P_2^+P_1C^-$. Furthermore, the linker lengths and positions have only little effect on the energy levels of the CS states: the energies are slightly higher for triad **P_2t9P_1C**, but the difference in the energies of the two states is roughly the same (0.04−0.05 eV) for both free-base triads. Instead, for **ZnP_2t9P_1C**, the reaction is exergonic with $-\Delta G = 0.3$ eV and it can be expected that the final CS state $ZnP_2^+P_1C^-$ will be reached before relaxation to the ground state.

The reduction peak of the **H_2P** reference is at about −1.2 V (Figure 3). The voltammograms of both **ZnP_2t9P_1C** and **P_2t9P_1C** have peaks approximately at this same potential. Therefore, it can be concluded that these peaks correspond to the reduction of free-base porphyrin also in the triads. This is

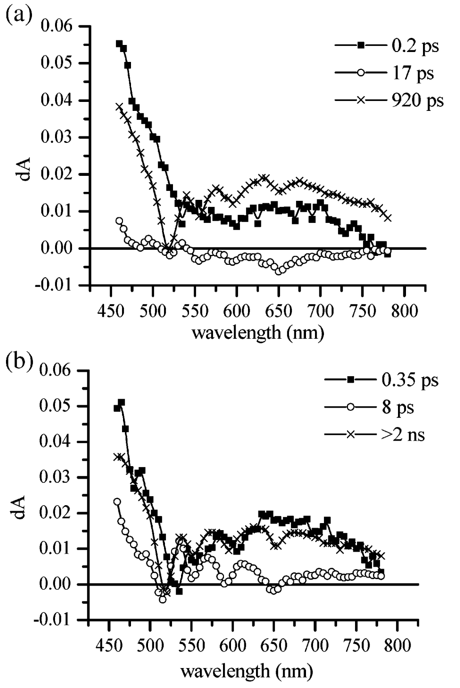

Figure 4. Decay component spectra of **P_2c10P_1C** in (a) PhCN and (b) toluene.

supported by the reported reduction potentials for C_{60}-fullerene by Dietel et al.:[4c] −1.015, −1.380, −1.85, and −2.310 V (vs Fc/Fc$^+$). The first two peaks of C_{60} can be seen in the voltammograms in Figure 3 measured for the triads as well, but between there is the additional peak at −1.23 V, which is attributed to the reduction of free-base porphyrin. For **P_2t9P_1C**, the peak is more intense, because the compound contains two free-base porphyrin moieties, whereas **ZnP_2t9P_1C** contains only one.

The energy of the CS state $ZnP_2{}^+P_1{}^-C$ can be calculated from the difference between the reduction peak of free-base porphyrin and the oxidation peak of Zn porphyrin. This energy is about 2.01 eV as is given in Table 2. This accounts for $-\Delta G = 0.04$ eV for the transition $ZnP_2^*P_1C$ (2.05 eV, Table 1) → $ZnP_2{}^+P_1{}^-C$, but here the solvent reorganization energy of the ion pair and Coulombic interactions are not taken into account, so the actual $-\Delta G$ is higher. Instead, the transition $ZnP_2P_1^*C$ → $ZnP_2{}^+P_1{}^-C$ is energetically unfavorable: the energy of $ZnP_2P_1^*C$ (1.90 eV, Table 1) is lower than that of $ZnP_2{}^+P_1{}^-C$.

3.3. Time-Resolved Measurements. *3.3.1. Transient Absorption Measurements.* The pump−probe method was used to measure the time-resolved absorptions of the compounds. The transient absorption decay curves obtained from the experimental data were fitted to a sum of exponentials.

The excitation wavelength of about 420 nm (Soret band) used for the pump−probe measurements of the free-base triads corresponds to the maximum absorption of the samples and populates the second excited singlet state of one of the porphyrin moieties in the molecule. This excited state decays so rapidly to the first excited singlet state that it cannot be observed in the measurements, but the formed first excited singlet state of porphyrin is detectable.

The porphyrin radical cation band[10] around 600−700 nm was seen for both of the free-base triads in PhCN (**P_2c10P_1C** as an example in Figure 4a) designating the formation of a CS state, which is most probably $P_2P_1{}^+C^-$ in the cases of **P_2t9P_1C** and **P_2c10P_1C** because porphyrins in these triads are the same and therefore ET between them is not expected. Also the DPV measurements showed that the transition $P_2P_1{}^+C^- \rightarrow P_2{}^+P_1C^-$ is energetically unfavorable. This is in agreement with the pump−probe results, where three exponents were enough to fit the results for the free-base triads suggesting the formation of the CS state $P_2P_1{}^+C^-$ via an exciplex and finally relaxation to the ground state. The lifetime of the CS state is about 900 ps for both free-base triads. Considering the characteristic fullerene radical anion absorption around 900 and 1000 nm,[11] the results obtained for all of the double-bridged triads are consistent with the corresponding dyads:[3] there is no noticeable band at 1000 nm, but the broad band at 900 nm, with similar time profile compared to the porphyrin radical cation band, can be attributed to the C_{60} radical anion (see Figure S2 for **ZnP_2t9P_1C** as an example).

In toluene (Figure 4b), the pump−probe measurements indicated the formation of an exciplex $P_2(P_1C)^*$ as the final state before relaxation to the ground state. When panels a and b of Figure 4 are compared, the shape of the final component, that is the CS state or the exciplex, is very similar. However, one can distinguish between the two states by considering the component preceding the final state. In PhCN (Figure 4a), the component with a lifetime of 17 ps has a negative amplitude at 650 nm indicating evidently the formation of a state, i.e. the CS state, whereas the component with a lifetime of 8 ps in toluene (Figure 4b) shows decay of the singlet excited state of porphyrin as bleaching of the Q-bands. Moreover, the long lifetime of the final state in toluene points to the exciplex, as intense exciplex emission was observed in the steady-state measurements (Figure S1).

In the case of the triad **ZnP_2t9P_1C**, the progress of the energy and electron-transfer reactions may depend on which one of the porphyrins in the triad is excited. Although at the Soret band both porphyrins of the triad are excited, in the Q-band region, the Zn and free-base porphyrin moieties absorb differently. To study this further, the reference compounds **ZnP**, **H_2P**, and **ZnP_2P_1** were investigated. The steady-state absorption spectrum of the porphyrin dyad indicates an exciton coupling between the parallel porphyrin chromophores:[12,13] the absorption of the dyad is clearly weaker than the sum of its components, and the Soret band is slightly shifted to the blue (see Figure S3a). To estimate the relative amounts of free-base porphyrins and zinc porphyrins excited at each wavelength, the relative absorption of free-base porphyrin in the dyad or triad containing both porphyrin moieties was calculated from the spectra of the porphyrin references (Figure S3b). This was done by dividing the spectrum of **H_2P** by the sum spectrum of **H_2P** and **ZnP**. The spectrum revealed that at 515 nm roughly 80% of the excited chromophores are free-base porphyrins. Similarly at 555 nm, 70% of the excited moieties are Zn porphyrins. Thus, to study more carefully the first steps of the ET reaction in triad **ZnP_2t9P_1C**, pump−probe measurements of the triad and the reference dyad **ZnP_2P_1** were carried out with the excitation wavelengths 515 and 555 nm populating the first excited singlet state of one of the porphyrins.

For the dyad **ZnP_2P_1** a two-exponential fit was enough for the samples in both solvents when excitation was carried out at 515 nm (see the Supporting Information Figure S4, in PhCN), but three exponents were needed for the spectra obtained with the excitation wavelength 555 nm (Figure 5, in PhCN). The results were very similar in both solvents.

It is clear from the bleaching of the corresponding Q-bands of the calculated spectra at 0 delay time (Figures 5b and S4b) that at 555 nm mostly Zn porphyrin (P_2) and at 515 nm free-base porphyrin (P_1) moieties are excited. From Figure 5b, one

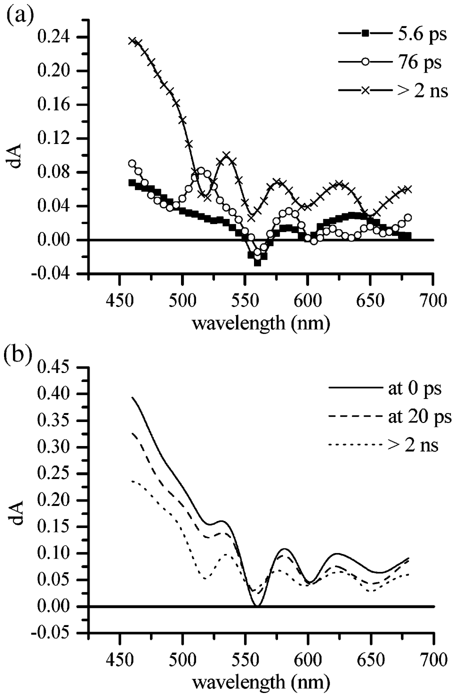

Figure 5. Transient absorption spectra of $\mathbf{ZnP_2P_1}$ in PhCN, excitation at 555 nm. (a) Decay component spectra and (b) calculated spectra at different delay times.

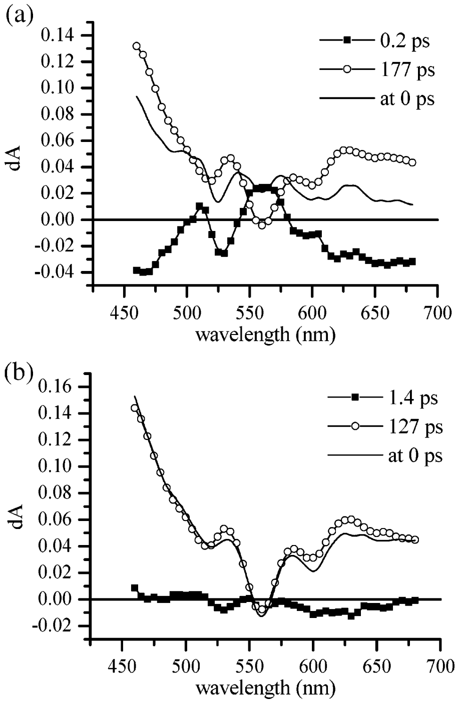

Figure 6. Decay component spectra and calculated spectrum at 0 delay time for $\mathbf{ZnP_2t9P_1C}$ in PhCN. (a) Excitation at 515 nm and (b) excitation at 555 nm.

can clearly see the energy transfer from excited P_2 to P_1: the bleaching of the band at 515 nm indicates the formation of excited free-base porphyrin with the simultaneous recovering of the Zn porphyrin band at 555 nm. The component with a lifetime of roughly 80 ps (Figure 5a) can be attributed to the energy transfer. In the measurement with the excitation at 515 nm, no energy transfer was observed as expected, but only the decay of excited free-base porphyrin with a lifetime of about 10 ns, which is above the range of the instrument. However, an additional short component (with a lifetime of roughly 6 and 17 ps in measurements at 555 and 515 nm, respectively) with the same shape was resolved in measurements with both excitation wavelengths. This might be due to some interaction state between the two porphyrins, but this state has not yet been identified.

The component spectra of $\mathbf{ZnP_2t9P_1C}$ in PhCN are shown in Figure 6, panels a and b, with excitations at 515 and 555 nm. The calculated spectra at 0 delay time are given in the same figures. A very fast component is observed for the triad when exciting mainly the free-base porphyrin moiety P_1 at 515 nm. The shape of the component indicates that Zn porphyrin is already involved in the reaction (band around 560 nm) and that porphyrin radicals are formed (a broad band with negative amplitude at longer than 580 nm). Furthermore, formation of the fullerene radical anion band with a comparable time constant was observed at 900 nm (Figure S2a). These features suggest ET to yield the complete CS state $ZnP_2^+P_1C^-$ in about 200 fs. Actually, the existences of free-base porphyrin as an exciplex $ZnP_2(P_1C)^*$ or as the CS state $ZnP_2P_1^+C^-$ are not indicated by any of the decay components, and only the formation of the complete CS state is resolved. Because of the extremely rapid electron-transfer yielding the complete CS state, the possible intermediates of the reaction cannot be resolved with the instrument.

When mostly the Zn porphyrin is excited (Figure 6b), the amplitude of the short component is very weak and therefore the indicated lifetime is not accurate. Thus, it is hard to say what happens directly after the excitation of P_2 in this triad. Still, the negative amplitudes of the broad bands around 600−650 and 900 nm (Figure S2b) refer to the same phenomenon as with excitation at 515 nm, namely formation of the complete CS state $ZnP_2^+P_1C^-$. However, when the Zn porphyrin is excited, one would expect first slow energy transfer to the free-base porphyrin, like observed for the corresponding dyad (component with a lifetime of roughly 80 ps, Figure 5a). Such a component is not seen for the triad. Therefore, the path to the final CS state seems to be different depending on which porphyrin of the triad is excited.

Regardless of whether free-base or Zn porphyrin (Figure 6, excitation at 515 or 555 nm) is excited, a component with a lifetime between 130 and 180 ps is observed. This component has the same shape with both of the excitation wavelengths. Consistently, the band at 900 nm attributed to fullerene anion decays with a lifetime of 140 ps regardless of the excitation wavelength (Figure S2). Thus, it seems reasonable to attribute this lifetime to correspond to the relaxation of $ZnP_2^+P_1C^-$ to the ground state. As a conclusion, one can state that the CS state of $\mathbf{ZnP_2t9P_1C}$ is formed in PhCN extremely rapidly regardless of which porphyrin is excited and it lives for about 150 ps.

The component spectra of $\mathbf{ZnP_2t9P_1C}$ in toluene are shown in Figure 7, panels a and b, for excitations at 515 and 555 nm, respectively. The calculated spectra at 0 delay time are given in the same figures. Also in toluene, two exponents were enough in the fitting for the results of both excitation wavelengths.

Figure 7 reveals that in toluene solution of the triad no fast components were resolved. However, the bands around 550 nm indicate that Zn porphyrin is involved in this reaction as well from the very beginning to the end and the broad bands around 600−650 nm again suggest the presence of the porphyrin radicals. This indicates similar reaction paths as were determined in PhCN. The bands around 600−650 nm are essentially the same for both excitation wavelengths, even though the lifetimes are different. Therefore, we can conclude that stepwise ET

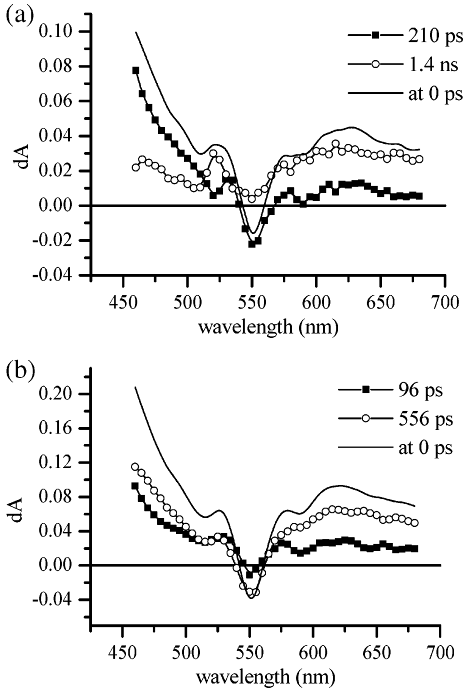

Figure 7. Decay component spectra and calculated spectrum at 0 delay time for **ZnP$_2$t9P$_1$C** in toluene. (a) Excitation at 515 nm and (b) excitation at 555 nm.

forming the final CS state ZnP$_2^+$P$_1$C$^-$ takes place no matter which porphyrin is excited. The lifetime of the CS state obtained from the measurements at excitation wavelength of 555 nm is more reliable, because the signal was much stronger than in the measurements at 515 nm. The reason for the weaker signal at 515 nm is the lower absorbance of the sample at this wavelength compared to 555 nm. In toluene another shorter component with a similar shape to that of the longer component was resolved as well. The shape of the component refers to a CS state, thus this could be an intermediate CS state via which the complete CS state is formed. The character of this state will be discussed in more detail in the Conclusions section.

3.3.2. Fluorescence Decays with Up-Conversion. The fluorescence up-conversion method was used to measure especially the fastest components of the fluorescence decay of the triads. The excitation wavelengths used were 405−430 nm where both porphyrin moieties of the triads absorb. The measurements were followed at 600−610 or 650−660 nm depending on the emission maxima of each triad. The absorption spectra recorded before and after the up-conversion measurements revealed that two of the samples (**P$_2$c10P$_1$C** in PhCN and **P$_2$t9P$_1$C** in toluene) were degraded by the excitation light in the measurements. Results from these measurements were not used to determine the lifetimes of the reaction, but results of the pump−probe measurements were utilized instead.

The fluorescence decays were quite similar for triads **P$_2$c10P$_1$C** and **P$_2$t9P$_1$C** in both solvents. As an example the decay curves of **P$_2$t9P$_1$C** in PhCN in two different time scales are presented in Figure 8, panels a and b. In a shorter time scale, a very fast component with a lifetime of approximately 0.2 ps was observed. In addition, two longer-lived components were resolved in the longer time scale. Based on the measurements of the corresponding dyads,[3] the fast component was attributed to the rapid relaxation of the excited P$_1$ to the exciplex. Thus, the longer-lived components are due to the decay of P$_2$. One possible reason for the two longer lifetimes instead of just one is the coexistence of two conformers of the triad with different distances between the porphyrin rings resulting in different rates of the energy transfer from the excited P$_2$.

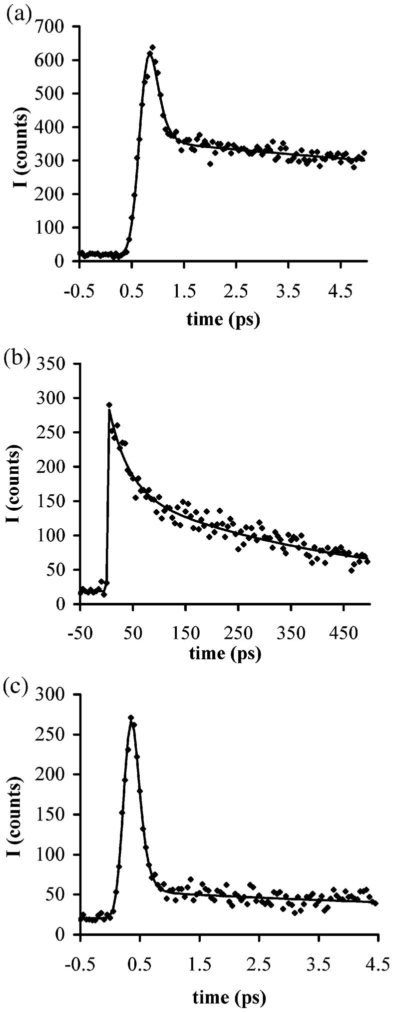

Figure 8. Fluorescence decay curves. (a) and (b) **P$_2$t9P$_1$C** in PhCN at 655 nm in two different time scales. The excitation was carried out at 420 nm. (c) **ZnP$_2$t9P$_1$C** in toluene at 600 nm. The excitation was carried out at 427 nm.

Rather different behavior was observed for triad **ZnP$_2$t9P$_1$C**. When emission was monitored at 600 or 610 nm, where only Zn porphyrin P$_2$ emits, a very fast component was observed. This component covers the decay almost completely and there are no significant longer-lived components such as there were for the other triads. Also when emission was monitored at 660 nm, the fast component had a higher amplitude compared to what was measured for the other triads. These observations show that singlet excited states of both porphyrins of **ZnP$_2$t9P$_1$C** relax very rapidly to some following transient states.

The time constant of the energy transfer from Zn porphyrin P$_2$ to free-base porphyrin P$_1$ was determined as 80 ps in the pump−probe measurements of the corresponding porphyrin dyad **ZnP$_2$P$_1$**. The 0.1 ps lifetime measured with the up-conversion at roughly 600 nm for triad **ZnP$_2$t9P$_1$C** is too short to be just this energy transfer. The pump−probe measurements with the excitation wavelengths of 515 and 555 nm revealed that there is ET from P$_2$ to P$_1$C. The very short lifetimes obtained from the pump−probe and up-conversion measurements in PhCN correlate well. However, with the up-conversion, the short component was observed at 600 nm also in toluene, whereas in the pump−probe, this short component was not resolved. Thus, it seems that rapid charge separation indeed takes place even in nonpolar toluene.

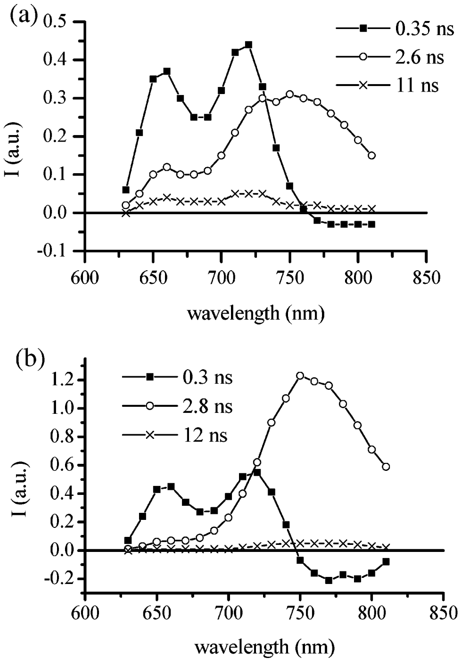

Figure 9. Decay-associated spectra of (a) **P_2c10P_1C** and (b) **P_2t9P_1C** in toluene.

3.3.3. Time-Correlated Single Photon Counting. Since the time scales of the up-conversion and pump−probe equipments were not sufficient to cover completely the decay of the free-base triads in toluene, the time-correlated single photon counting method was used to resolve the longer lifetimes. The excitation wavelength in these measurements was 590 nm resulting in the first excited singlet state of one of the molecule's porphyrins.

The decay-associated spectra (DAS) of the triads **P_2c10P_1C** and **P_2t9P_1C** in toluene are presented in Figure 9. Comparison of the DAS of **P_2c10P_1C** and **P_2t9P_1C** reveals that the shapes of the spectra are very similar, but the intensities of the components are different. The components with lifetimes of about 0.3 ns for both of the triads are the combination of the porphyrin emissions as P_2 transfers its energy to P_1 and the formation of the exciplex from the excited P_1. This slow energy transfer is in agreement with the long lifetimes measured for the decay of P_2 in up-conversion (Figure 8). The 2.6−2.8 ns component is evidently the exciplex emission. For **P_2t9P_1C**, the exciplex emission is clearly stronger than the porphyrin monomer emission, whereas for **P_2c10P_1C**, the porphyrin monomer emission has a higher intensity. This is a distinct indication that in **P_2t9P_1C**, where the trans positions of the linkers make the structure more stable, the energy transfer from P_2 to P_1 occurs more efficiently. Taking into account the characteristic lifetimes and the weak amplitudes of the longest-lived components of Figure 9, these components can be designated to some minor **H_2P** monomer impurities in the samples.

4. Conclusions

The simplified Schemes 2 and 3 can be suggested for reactions of triads **P_2t9P_1C** and **P_2c10P_1C** in nonpolar and in polar environments, respectively. For the free-base triads, there is no evidence of charge separation in toluene, but the exciplex relaxes directly to the ground state. However, the time-resolved spectroscopic studies indicate that a CS state is formed in PhCN. Thus, it can be assumed that in PhCN the energy of $P_2P_1^+C^-$ lies somewhat lower than that of the exciplex. The formation of the final CS state was not observed as expected based on the DPV measurements. The steady-state fluorescence measurements proved that the energy transfer between the porphyrins P_2 and P_1 is less efficient for **P_2c10P_1C** than for **P_2t9P_1C**, but in general the same reaction schemes can be suggested for both free-base triads. Except for the energy transfer from P_2 to P_1 these schemes are essentially the same as the ones suggested for the corresponding dyad[3].

SCHEME 2: Reaction Scheme for Triads P_2t9P_1C and P_2c10P_1C in Toluene

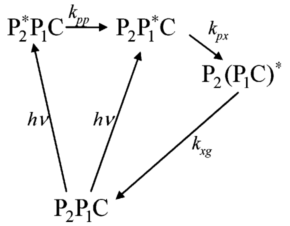

SCHEME 3: Reaction Scheme for Triads P_2t9P_1C and P_2c10P_1C in PhCN

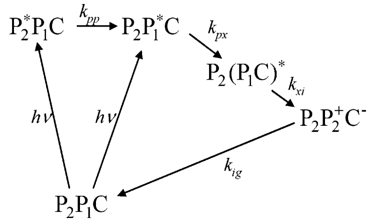

SCHEME 4: Reaction Scheme for Triad ZnP_2t9P_1C[a]

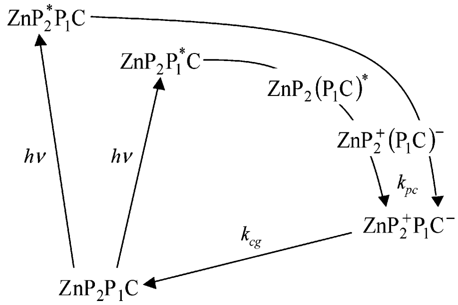

[a] k_{pc} is the rate constant for the transitions from the locally excited states of P_2 or P_1 to the complete CS state $ZnP_2^+P_1C^-$. The two intermediates given were not well identified in the measurements; see the text for discussion.

Scheme 4 can be suggested for triad **ZnP_2t9P_1C** both in PhCN and in toluene. In **ZnP_2t9P_1C**, the energies of the states determined from the steady-state fluorescence and DPV measurements are clearly different, and it can be expected that there is formation of the complete CS state $ZnP_2^+P_1C^-$. The pump−probe measurements done with the excitation wavelengths 515 and 555 nm showed that the CS state $ZnP_2^+P_1C^-$ is formed extremely rapidly regardless of which porphyrin is excited and in both polar and nonpolar solvents. Since the complete CS state is formed so fast after the excitation, the possible transients leading to this state cannot be identified from the measurements. The intermediates given in Scheme 4 are just guesses based on the very different behavior of the triad compared to the **ZnP_2P_1** dyad in the pump−probe measurements suggesting that P_1 and C in the triad act as a single moiety P_1C. This is reasonable taking into account the ground state and excited-state interaction of the corresponding porphyrin−fullerene dyad[3] observed as visible changes in the absorption and emission properties compared to the individual chromophores.

TABLE 3: Rate Constants (s^{-1}) for the Triads P_2c10P_1C and P_2t9P_1C and the Reference Dyad P_1C[3] [a]

compound	solvent	k_{pp}	k_{px}	k_{xg}	k_{xi}	k_{ig}
P_1C	toluene		6×10^{12}	0.34×10^9		
P_2c10P_1C	toluene	59×10^{9b} 4×10^{9b}	5×10^{12b}	0.38×10^{9c}		
P_2t9P_1C	toluene	26×10^9	5×10^{12}	0.36×10^{9c}		
P_1C	PhCN		10×10^{12}		1.0×10^{11}	2.6×10^9
P_2c10P_1C	PhCN	$\sim 100 \times 10^9$	7×10^{12b}		$\sim 1 \times 10^{11}$	1.1×10^9
P_2t9P_1C	PhCN	27×10^{9b} 2.2×10^{9b}	6.7×10^{12b}		$\sim 1 \times 10^{11}$	1.1×10^9

[a] k_{pp} = energy transfer from P_2 to P_1, k_{px} = formation rate of the exciplex $P_2(P_1C)^*$, k_{xg} = relaxation rate of the exciplex, k_{xi} = formation rate of the CS state $P_2P_1^+C^-$, k_{ig} = relaxation rate of the CS state $P_2P_1^+C^-$. [b] From the up-conversion measurements. [c] From the TCSPC measurements.

TABLE 4: Rate Constants (s^{-1}) for ZnP_2t9P_1C and the Reference Dyad ZnP_1C (the same as P_1C but with Zn as the Center Atom of Porphyrin)[3] [a]

compound	solvent	k_{pc}	k_{cg}
ZnP_1C	PhCN		16×10^9
ZnP_2t9P_1C	toluene	10×10^{12b}	1.8×10^9
	PhCN	10×10^{12b}	6.6×10^9

[a] k_{pc} = formation rate of the final CS state $ZnP_2^+P_1C^-$ from excited P_2 or P_1, k_{cg} = relaxation rate of the final CS state $ZnP_2^+P_1C^-$. [b] From the up-conversion measurements.

Based on the steady-state emission spectrum of the triad in toluene, we can assume that the exciplex is formed when free-base porphyrin P_1 is excited, but that this state also relaxes rapidly. The pump−probe component spectra showed that Zn porphyrin P_2 is involved in the reaction already 0.2 ps after excitation even when mostly P_1 is excited so the state following the exciplex is most probably a CS state in which P_2 holds the positive charge. Taking into account that ET occurs so rapidly, the negative charge could first be delocalized around P_1 and C, i.e., in a state denoted as $ZnP_2^+(P_1C)^-$. The complete CS state $ZnP_2^+P_1C^-$ follows this $ZnP_2^+(P_1C)^-$ state. The pump−probe measurements in toluene revealed a transient state preceding the final CS state also with CS state characteristics and a lifetime of roughly 100−200 ps depending on the excitation wavelength (Figure 7). This might be the intermediate CS state $ZnP_2^+(P_1C)^-$. Another explanation for this intermediate could be the CS state $ZnP_2^+P_1^-C$ between the two porphyrins, but the pump−probe measurements of the corresponding dyad **ZnP_2P_1** do not support this idea: no ET was observed for the dyad. A different path is more probable when Zn porphyrin P_2 is excited. Since the pump−probe measurements proved that the energy transfer does not take place in this triad, the exciplex will not be formed either. Instead, it’s likely that the complete CS state $ZnP_2^+P_1C^-$ is formed just via $ZnP_2^+(P_1C)^-$.

The rate constants of the transitions of the ET reaction for the triads and the corresponding dyads are summarized in Table 3 for the free-base triads **P_2c10P_1C** and **P_2t9P_1C** and in Table 4 for **ZnP_2t9P_1C**.

In toluene, the free-base triads **P_2c10P_1C** and **P_2t9P_1C** behave very similarly to the dyad **P_1C**. The lifetimes for the exciplex formation and relaxation are approximately the same for all of these compounds. Also in PhCN, the exciplex and the CS state are formed with equal rates, but the CS state $P_2P_1^+C^-$ of the free-base triads lasts over two times longer than the CS state of the dyad **P_1C**. This could be because of a shielding effect that P_2 might have on the P_1^+ by not allowing the solvent molecules to approach the cation. In addition, there is an energy transfer between the two porphyrins of the triad molecules. The energy transfer of the free-base triads is biexponential, as mentioned in connection with the up-conversion results, which makes the comparison of energy transfer rates of the two triads difficult. It should also be taken into account that the energy transfer rates of Table 3 are obtained from two different measurements, up-conversion and pump−probe. The rates from up-conversion are more accurate, but for some of the samples reliable results were not obtained from these measurements. Thus, rates from the pump−probe results are given as indicated in the table.

Comparing the rate constants of **ZnP_2t9P_1C** in Table 4 and those of **P_1C** in Table 3, one notices that the complete CS state of **ZnP_2t9P_1C** is formed a 100 times faster than the CS state of the dyad, but it also relaxes about 2.5 times faster in PhCN. In this comparison, it is clear that the increase in charge separation distance does not result in the increase of the lifetime of the CS state. The reason for this can be a lower energy of the CS state which should lead to a shorter lifetime in the Marcus inverted region. Actually, the CS state lifetime of the triad is still a few times longer than that of the **ZnP_1C** dyad (Table 4), which is otherwise the same as the dyad **P_1C**, but contains Zn as the center atom of porphyrin, and is expected to have similar CS state energetics to the triad. So increase in the charge separation distance results in increase of the CS state lifetime, indeed.

A longer lifetime of the CS state is observed in toluene. Although we have no direct measurements of the CS state energy (DPV measurements were not possible in toluene), there is a hint indicating that the energy of this state in toluene is close to that of the exciplex. According to our interpretation of the pump−probe data, the exciplex $ZnP_2(P_1C)^*$ is quenched efficiently by the fast charge separation. Nevertheless, some residual exciplex emission was observed with relative intensity roughly 12 times lower than that of the dyad. This is possible if the exciplex and the CS state $ZnP_2^+P_1C^-$ or $ZnP_2^+(P_1C)^-$ are in equilibrium shifted gradually to the side of the CS state. In such a case, the energy of the CS state is lower than the energy of the exciplex by 2kT roughly; that is, it is close to 1.7 eV. The difference in the energies of the CS states in PhCN and toluene, 0.3 eV, seems to be reasonable taking into account the relatively big charge separation distance for the triad.

Acknowledgment. This work was supported by the project Organic Structures as Photoactive Materials of the Academy of Finland.

Supporting Information Available: Emission spectra of triads **P_2c10P_1C** and **P_2t9P_1C** in toluene, transient absorption spectra of **ZnP_2t9P_1C** in PhCN recorded at 850−1070 nm, absorption spectra of the reference compounds **H_2P**, **ZnP** and **ZnP_2P_1** in toluene, the relative absorption of free-base porphyrin compared to Zn porphyrin at the Q-band region and the transient absorption spectra of **ZnP_2P_1** in PhCN with the excitation wavelength of 515 nm. This material is available free of charge via the Internet at http://pubs.acs.org.

References and Notes

(1) (a) Marcus, R. A. *Rev. Mod. Phys.* **1993**, *65*, 599−610. (b) Bolton, J. R.; Archer, M. D. *Adv. Chem. Ser.* **1991**, *228*, 7−23.

(2) (a) Frey, W.; Klann, R.; Laermer, F.; Elsaesser, T.; Baumann, E.; Futscher, M.; Staab, H. A. *Chem. Phys. Lett*. **1992**, *190*, 567−573. (b) Häberle, T.; Hirsch, J.; Pöllinger, F.; Heitele, H.; Michel-Beyerle, M. E.; Anders, C.; Döhling, A.; Krieger, C.; Ruckemann, A.; Staab, H. A. *J. Phys. Chem.* **1996**, *100*, 18269−18274. (c) Imahori H.; Tkachenko, N. V.; Vehmanen, V.; Tamaki, K.; Lemmetyinen, H.; Sakata, Y.; Fukuzumi, S. *J. Phys. Chem. A* **2001**, *105*, 1750−1756.

(3) Chukharev, V.; Tkachenko, N. V.; Efimov, A.; Guldi, D. M.; Hirsch, A.; Scheloske, M.; Lemmetyinen, H. *J. Phys. Chem. B* **2004**, *108*, 16377−16385.

(4) (a) Imahori H.; Hagiwara, K.; Aoki, M.; Akiyama, T.; Taniguchi, S.; Okada, T.; Shirakawa, M.; Sakata, Y. *J. Am. Chem. Soc.* **1996**, *118*, 11771−11782. (b) Kuciauskas, D.; Lin, S.; Seely, G. R.; Moore, A. L.; Moore, T. A.; Gust, D.; Drovetskaya, T.; Reed, C. A.; Boyd, P. D. W. *J. Phys. Chem.* **1996**, *100*, 15926−15932. (c) Dietel, E.; Hirsch, A.; Zhou, J.; Rieker, A. *J. Chem. Soc., Perkin Trans. 2* **1998**, *6*, 1357−1364. (d) Yamada, K.; Imahori, H.; Nishimura, Y.; Yamazaki, I.; Sakata, Y. *Chem. Lett.* **1999,** 895−896. (e) Imahori, H.; El-Khouly, M. E.; Fujitsuka, M.; Ito, O.; Sakata, Y.; Fukuzumi, S. *J. Phys. Chem. A* **2001**, *105*, 325−332. (f) D'Souza, F.; Gadde, S.; Zandler, M. E.; Arkady, K.; El-Khouly, M. E.; Fujitsuka, M.; Ito, O. *J. Phys. Chem. A* **2002**, *106*, 12393−12404. (g) Kesti, T. J.; Tkachenko, N. V.; Vehmanen, V.; Yamada, H.; Imahori, H.; Fukuzumi, S.; Lemmetyinen, H. *J. Am. Chem. Soc.* **2002**, *124*, 8067−8077. (h) Tkachenko, N. V.; Lemmetyinen, H.; Sonoda, J.; Ohkubo, K.; Sato, T.; Imahori, H.; Fukuzumi, S. *J. Phys. Chem. A* **2003**, *107*, 8834−8844. (i) Fukuzumi, S.; Imahori, H.; Yamada, H.; El-Khouly, M. E.; Fujitsuka, M.; Ito, O.; Guldi, D. M. *J. Am. Chem. Soc.* **2001**, *123*, 2571−2575. (j) Imahori, H.; Tamaki, K.; Guldi, D. M.; Luo, C.; Fujitsuka, M.; Ito, O.; Sakata, Y.; Fukuzumi, S. *J. Am. Chem. Soc.* **2001**, *123*, 2607−2617. (k) D'Souza, F.; Deviprasad, G. R.; Zandler, M. E.; El-Khouly, M. E.; Fujitsuka, M.; Ito, O. *J. Phys. Chem. B* **2002**, *106*, 4952−4962.

(5) (a) Liddell, P. A.; Kuciauskas, D.; Sumida, J. P.; Nah, B.; Nguyen, D.; Moore, A. L.; Moore, T. A.; Gust, D. *J. Am. Chem. Soc.* **1997**, *119*, 1400−1405. (b) Kuciauskas, D.; Liddell, P. A.; Lin, S.; Johnson, T. E.; Weghorn, S. J.; Lindsey, J. S.; Moore, A. L.; Moore, T. A.; Gust, D. *J. Am. Chem. Soc.* **1999**, *121*, 8604−8614. (c) Tamaki, K.; Imahori, H.; Sakata, Y.; Nishimura, Y.; Yamazaki, I. *Chem. Commun*. **1999**, *7*, 625−626. (d) Fujitsuka, M.; Ito, O.; Imahori, H.; Yamada, K.; Yamada, H.; Sakata, Y. *Chem. Lett.* **1999**, 721−722. (e) Luo, C.; Guldi, D. M.; Imahori, H.; Tamaki, K.; Sakata, Y. *J. Am. Chem. Soc.* **2000**, *122*, 6535−6551. (f) Imahori, H.; Guldi, D. M.; Tamaki, K.; Yoshida, Y.; Luo, C.; Sakata, Y.; Fukuzumi, S. *J. Am. Chem. Soc.* **2001**, *123*, 6617−6628. (g) Imahori, H.; Tamaki, K.; Araki, Y.; Sekiguchi, Y.; Ito, O.; Sakata, Y.; Fukuzumi, S. *J. Am. Chem. Soc*. **2002**, *124*, 5165−5174. (h) Kodis, G.; Liddell, P. A.; de la Garza, L.; Clausen, P. C.; Lindsey, J. S.; Moore, A. L.; Moore, T. A.; Gust, D. *J. Phys. Chem. A* **2002**, *106*, 2036−2048. (i) Guldi, D. M.; Imahori, H.; Tamaki, K.; Kashiwagi, Y.; Yamada, H.; Sakata, Y.; Fukuzumi, S. *J. Phys. Chem. A* **2004**, *108*, 541−548. (j) Liddell, P. A.; Kodis, G.; de la Garza, L.; Moore, A. L.; Moore, T. A.; Gust, D. *J. Phys. Chem. B* **2004**, *108*, 10256−10265. (k) D'Souza, F.; Smith, P. M.; Gadde, S.; McCarty, A. L.; Kullman, M. J.; Zandler, M. E.; Itou, M.; Araki, Y.; Ito, O. *J. Phys. Chem. B* **2004**, *108*, 11333−11343.

(6) (a) Dietel, E.; Hirsch, A.; Eichhorn, E.; Rieker, A.; Hackbarth, S.; Roder, B. *Chem. Commun.* **1998**, 1981−1982. (b) Schuster, D. I.; Cheng, P.; Wilson, S. R.; Prokhorenko, V.; Katterle, M.; Holzwarth, A. R.; Braslavsky, S. E.; Klihm, G.; Williams, R. M.; Luo, C. *J. Am. Chem. Soc.* **1999**, *121*, 11599−11600. (c) Guldi, D. M.; Luo, C.; Da Ros, T.; Prato, M.; Dietel, E.; Hirsch, A. *Chem. Commun.* **2000**, 375−376. (d) Schuster, D. I.; Cheng, P.; Jarowski, P. D.; Guldi, D. M.; Luo, C.; Echegoyen, L.; Pyo, S.; Holzwarth, A. R.; Braslavsky, S. E.; Williams, R. M.; Klihm, G. *J. Am. Chem. Soc.* **2004**, *126*, 7257−7270.

(7) Efimov, A.; Vainiotalo, P.; Tkachenko, N.; Lemmetyinen, H. *J. Porphyrins Phthalocyanines* **2004**, *7*, 610−616.

(8) (a) Tkachenko, N. V.; Grandell, D.; Ikonen, M.; Jutila, A.; Moritz, V.; Lemmetyinen, H. *Photochem. Photobiol*. **1993**, *58*, 284−289. (b) Vehmanen, V.; Tkachenko, N. V.; Imahori, H.; Fukuzumi, S.; Lemmetyinen, H. *Spectrochim. Acta A* **2001**, *57*, 2229−2244.

(9) Tkachenko, N. V.; Rantala, L.; Tauber, A. Y.; Helaja, J.; Hynninen, P. H.; Lemmetyinen, H. *J. Am. Chem.* Soc. **1999**, *121*, 9378−9387.

(10) Gasyna, Z.; Browett, W. R.; Stillman, M. J. *Inorg. Chem.* **1985**, *24*, 2440−2447.

(11) Greaney, M. A.; Gorum, S. M. *J. Phys. Chem.* **1991**, *95*, 7142−7144.

(12) Kasha, M.; Rawls, H. R.; Ashraf El-Bayoumi, M. *Pure Appl. Chem*. **1965**, *11*, 371−392.

(13) (a) Osuka, A.; Maruyama, J. *J. Am. Chem. Soc.* **1988**, *110*, 4454. (b) Le Mest, Y.; L'Her, M.; Hendricks, N. H.; Kim, K.; Collman, J. P. *Inorg. Chem.* **1992**, *31*, 835−847. (c) Aratani, N.; Osuka, A.; Cho, H. S., Kim, D. *J. Photochem. Photobiol. C* **2002**, 3, 25−52. (d) Kim, D.; Osuka, A. *J. Phys. Chem. A* **2003**, *107*, 8791−8816.